Journal of Sound and Vibration 329 (2010) 4534–4549

Contents lists available at ScienceDirect

Journal of Sound and Vibration

journal homepage: www.elsevier.com/locate/jsvi

Domain-partition power series in vibration analysis of variable-cross-section rods

José A. Inaudi *, Ariel E. Matusevich

School of Engineering, National University of Córdoba, Casilla de correo 916, Córdoba 5000, Argentina

ARTICLE INFO

Article history:
Received 12 December 2009
Received in revised form
24 April 2010
Accepted 26 April 2010
Handling Editor: M.P. Cartmell

ABSTRACT

This paper presents a power series method with domain partition implemented in a matrix formulation, as an alternative to other power series techniques in vibration analysis. The proposed method solves linear differential equations efficiently up to a desired degree of accuracy and remedies two limitations of the conventional power series method. One limitation is related to the convergence domain of the series solution. If this domain does not include the region under analysis, the series expansion gives meaningless results. The other limitation is computational in nature; numerical difficulties arise when calculating natural frequencies, modes of vibration and dynamic stiffness of continuous models at high frequency. To compare some of the available implementations of the power series method in modal analysis, the longitudinal vibration of a rod with linearly varying area is studied. By means of this simple example, it is demonstrated that the power series method with domain partition provides more versatility than the power series approximation on complete domains.

1. Introduction

The Power Series Method (PSM) is a widely known technique for solving ordinary differential equations. This method is covered in most books on differential equations [1–4] and its origins can be traced back to the seventeenth century, when the foundations of differential and integral calculus were developed [3]. The basic approach of the PSM is to assume a solution in the form of infinite Taylor series, formally substitute this form into the differential equation and after algebraic manipulations, obtain recurrence relations for the series coefficients. In practical applications, the series expansion is truncated to a finite number of terms to approximate the solution up to some limiting accuracy. To mention only a couple of papers on this topic among a large number available in the literature, we can highlight Eisenberger [5] on the application of the PSM to the calculation of natural frequencies of variable-cross-section rods, and Zhu and Leung [6] on the computation of the dynamic stiffness of thin-walled structures by power series.

An alternative implementation of the PSM is known as Differential Transformation Method (DTM) [7]. In this method, the differential equations and boundary conditions (or the initial conditions depending on the problem) are transformed into a set of algebraic equations. PSM and DTM differ in the way of obtaining the recurrence equations, but are in essence of the same method. In both versions, the process of iteratively obtaining the series coefficients is typically systematised for each problem, using a symbolic manipulation program such as Maple® or Mathematica®. However, the formulation of the

* Corresponding author: Tel.: +54 9 351 5936097.
E-mail addresses: inaudijose@gmail.com (J.A. Inaudi), ariel.matusevich@gmail.com (A.E. Matusevich).

0022-460X/$ - see front matter © 2010 Elsevier Ltd. All rights reserved.
doi:10.1016/j.jsv.2010.04.028

recurrence relations is usually derived by hand. This disadvantage can be overcome, when the PSM is reformulated in terms of matrix operators.

The PSM is especially well suited for finding solutions of differential equations with varying coefficients. These equations typically arise in problems of vibrations, structural analysis, and heat transfer. The application of the PSM to the vibration analysis of continuous systems with variable parameters is seldom mentioned as an alternative in books on vibrations; the classical approach is finite element analysis or the Rayleigh–Ritz method. Accurate solutions may also be obtained using the PSM, because the polynomial function which approximates the deformation field satisfies the differential equation up to a desired degree and boundary conditions.

The PSM is not an infallible method and should not be used indiscriminately. A series solution converges in a region free of singularities; when singularities exist, the convergence is not guaranteed. The presence of singular points in the differential equation governs the existence and rate of convergence of the series solution [8]. In addition, numerical difficulties occur when using the PSM in the solution of modes of vibration, natural frequencies, and dynamic stiffness of continuum models at high frequency. These concepts and limitations are revisited in this work, and justify the proposed method of power series with the domain partition. The evaluation of the accuracy and computational efficiency of the method in comparison with Rayleigh–Ritz or finite element methods is beyond the scope of this work; this will be addressed in future research of the authors.

The paper is organised as follows. In Section 2, the boundary value problem of a tapered rod in axial vibration is presented and analysed using the implementations of the PSM, DTM, and PSM with domain partition. In Section 3, the computation of dynamic stiffness of a non-uniform rod is addressed. Using these examples as case studies, the advantages and disadvantages of the addressed power series techniques are illustrated. Finally, conclusions and directions for further research are presented.

2. Free vibration analysis of a tapered-rod

The axial displacement field of a rod is governed by the following partial differential equation [9]:

$$\frac{\partial}{\partial x}\left[EA(x)\frac{\partial}{\partial x}u(x,t)\right]-\rho A(x)\frac{\partial^2}{\partial t^2}u(x,t)=0 \tag{1}$$

E and ρ are the Young modulus and mass density of the rod material, $A(x)$ is the cross-sectional area, and $u(x,t)$ is the axial displacement field. In Fig. 1a and b, the origin of the coordinate system for variable x is placed at a distance γL from the left side of the rod, where L is the length of the rod and γ is a dimensionless parameter that can take any value between 0 and 1.

Using the method of separation of variables, the solution of Eq. (1) is assumed to be the product of a shape function $\phi(x)$ and a time varying amplitude $Y(t)$

$$u(x,t)=\phi(x)Y(t) \tag{2}$$

Substitution of Eq. (2) into Eq. (1) yields ordinary differential equations for $\phi(x)$ and $Y(t)$.

If we consider homogenous material properties and normalise the axial position coordinate x by the length of the rod

$$\xi=\frac{x}{L} \tag{3}$$

we obtain the following non-dimensional differential equation with varying coefficients for the shape functions

$$A\frac{d^2\phi}{d\xi^2}+\frac{dA}{d\xi}\frac{d\phi}{d\xi}+A\overline{\omega}^2\phi=0 \tag{4}$$

In Eq. (4), $\overline{\omega}$ is the dimensionless frequency given by

$$\overline{\omega}=\sqrt{\frac{\rho L^2}{E}}\omega \tag{5}$$

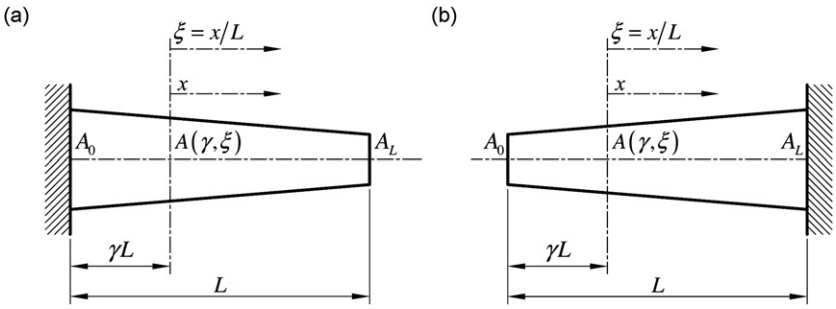

Fig. 1. (a) Clamped-free rod and (b) free-clamped rod.

and ω represents the frequency variable. The values of ω that provide solutions of Eq. (4) for the corresponding boundary conditions are the natural frequencies of the model ω_i (with i=1, 2, …, ∞).

When we consider a rod with linearly varying area, the area function $A(\gamma,\xi)$ takes the following form:

$$A(\gamma,\xi)=a\xi+b,\quad a=A_L-A_0,\quad b=A_0+(A_L-A_0)\gamma \tag{6}$$

In Eq. (6), A_0 and A_L are the cross-sectional areas on the left and right side of the rod, respectively. Introducing Eq. (6) into Eq. (4), the mode shape equation becomes:

$$(a\xi+b)\frac{d^2\phi}{d\xi^2}+a\frac{d\phi}{d\xi}+(a\xi+b)\overline{\omega}^2\phi=0 \tag{7}$$

The free vibration problem of a rod clamped at one end and free at the other can be solved as "clamped-free" or "free-clamped" (see Fig. 1a and b) depending on the coordinate system adopted. When the clamped-free problem is considered, the following conditions must be satisfied at the boundaries:

$$\phi(-\gamma)=0 \tag{8}$$

$$EA(1-\gamma)\frac{d\phi}{d\xi}(1-\gamma)=0\rightarrow\frac{d\phi}{d\xi}(1-\gamma)=0 \tag{9}$$

On the other hand, the free-clamped rod requires

$$EA(-\gamma)\frac{d\phi}{d\xi}(-\gamma)=0\rightarrow\frac{d\phi}{d\xi}(-\gamma)=0 \tag{10}$$

$$\phi(1-\gamma)=0 \tag{11}$$

In this section, we carry out the free vibration analysis of the clamped-free rod of Fig. 1a, using three implementations of the power series method: (i) the classical method of algebraic recurrences, (ii) the differential transformation method, and (iii) a matrix implementation. After that, we compare the power series solution of the clamped-free rod (Fig. 1a) with the solution of the free-clamped model (Fig. 1b). Then, we analyse the influence of a different centre of expansion in the convergence of the series solution. Finally, we present the method of power series with domain partition, a computational technique that enhances power series applicability.

2.1. Standard power series approach

According to the theory of power series [1], if ξ_0 is a regular point of Eq. (4), it is possible to derive a power series solution centred at ξ_0, which converges in a domain defined by

$$|\xi-\xi_0|<R \tag{12}$$

where R is the distance from ξ_0 to the nearest singular point. This distance, in the complex plane, represents the lower bound for the radius of convergence of the series solution.

If the series expansion is centred at the origin of the coordinate system, ξ_0=0. By moving this origin within the region under analysis, other points of expansion can be considered.

The power series solution defines a function whose domain is the interval of convergence of the series. Therefore, this domain must be large enough to include the element boundaries. If the element domain lies inside the region defined by Eq. (12), the existence of a power series solution can be assured.

Dividing both terms of Eq. (4) by the area function $A(\gamma,\xi)$, we obtain

$$\frac{d^2\phi}{d\xi^2}+\frac{1}{A}\frac{dA}{d\xi}\frac{d\phi}{d\xi}+\overline{\omega}^2\phi=0 \tag{13}$$

The mode shape equation expressed in this form – known as standard form – shows that the singular points of the differential equation are the zeros of the area function $A(\gamma,\xi)$, or its discontinuities, in which case the derivative of $A(\gamma,\xi)$ is not defined. For a rod with linearly varying area, there is only one singular point located at $\xi=-b/a$. Using Eq. (6), the lower bound for the radius of convergence is

$$R=\left|\frac{-b}{a}\right|=\left|\frac{A_0}{A_0-A_L}-\gamma\right| \tag{14}$$

As Eq. (14) indicates, the radius of convergence depends on two issues: (i) the geometry of the rod and (ii) the location of the origin of the coordinate system, where the series expansion is centred.

Let us consider the clamped-free rod of Fig. 1a. If the centre of the series expansion is placed on the left edge of the rod (γ=0)

$$A_0>A_L\rightarrow\frac{A_0}{A_0-A_L}>1\rightarrow R>1 \tag{15}$$

the convergence domain includes the region under analysis, assuring the convergence of the solution.

We propose the following power series expansion for the mode shape

$$\phi = \sum_{i=0}^{\infty} \lambda_i \xi^i \tag{16}$$

where λ_i are the unknown coefficients to be determined. Differentiation of Eq. (16) leads to

$$\frac{d\phi}{d\xi} = \frac{d}{d\xi}\left(\sum_{i=0}^{\infty} \lambda_i \xi^i\right) = \sum_{i=0}^{\infty} i\lambda_i \xi^{i-1} = \sum_{i=0}^{\infty} (i+1)\lambda_{i+1} \xi^i \tag{17}$$

$$\frac{d^2\phi}{d\xi^2} = \frac{d}{d\xi}\left(\sum_{i=0}^{\infty} (i+1)\lambda_{i+1} \xi^i\right) = \sum_{i=0}^{\infty} i(i+1)\lambda_{i+1} \xi^{i-1} = \sum_{i=0}^{\infty} (i+2)(i+1)\lambda_{i+2} \xi^i \tag{18}$$

Replacing Eqs. (16)–(18) in Eq. (7)

$$(a\xi+b)\sum_{i=0}^{\infty} (i+2)(i+1)\lambda_{i+2}\xi^i + a\sum_{i=0}^{\infty} (i+1)\lambda_{i+1}\xi^i + (a\xi+b)\overline{\omega}^2 \sum_{i=0}^{\infty} \lambda_i \xi^i = 0 \tag{19}$$

Expanding Eq. (19) and working out the resulting expression, we obtain

$$\sum_{i=1}^{\infty} \{b(i+2)(i+1)\lambda_{i+2} + a(i+1)^2\lambda_{i+1} + b\overline{\omega}^2\lambda_i + a\overline{\omega}^2\lambda_{i-1}\}\xi^i + 2b\lambda_2 + b\overline{\omega}^2\lambda_0 + a\lambda_1 = 0 \tag{20}$$

In order to satisfy the differential equation, the following terms in Eq. (20) must vanish:

$$2b\lambda_2 + b\overline{\omega}^2\lambda_0 + a\lambda_1 = 0 \tag{21}$$

$$b(i+2)(i+1)\lambda_{i+2} + a(i+1)^2\lambda_{i+1} + b\overline{\omega}^2\lambda_i + a\overline{\omega}^2\lambda_{i-1} = 0 \tag{22}$$

Assuming that b is non-zero, the following recurrence relations are obtained from Eqs. (21) and (22):

$$\lambda_2 = \frac{-a\lambda_1 - b\overline{\omega}^2\lambda_0}{2b} \tag{23}$$

$$\lambda_{i+2} = -\frac{a(i+1)^2\lambda_{i+1} + b\overline{\omega}^2\lambda_i + a\overline{\omega}^2\lambda_{i-1}}{b(i+2)(i+1)} \tag{24}$$

According to the boundary condition at $\xi = -\gamma = 0$

$$\phi(0) = 0 \rightarrow \sum_{i=0}^{\infty} \lambda_i 0^i = 0 \rightarrow \lambda_0 = 0 \tag{25}$$

Therefore, substituting Eq. (25) into Eq. (23)

$$\lambda_2 = \frac{-a}{2b}\lambda_1 \tag{26}$$

Using Eqs. (26) and (24), the coefficients of the series expansion can be obtained in terms of λ_1.

The following results were obtained for five successive coefficients:

$$i = 1, \quad \lambda_3 = \frac{2a^2 - b^2\overline{\omega}^2}{6b^2}\lambda_1 \tag{27}$$

$$i = 2, \quad \lambda_4 = \frac{-3a^3 + ab^2\overline{\omega}^2}{12b^3}\lambda_1 \tag{28}$$

$$i = 3, \quad \lambda_5 = \frac{24a^4 - 7a^2b^2\overline{\omega}^2 + b^4\overline{\omega}^4}{120b^2}\lambda_1 \tag{29}$$

$$i = 4, \quad \lambda_6 = \frac{-40a^5 + 11a^3b^2\overline{\omega}^2 - ab^4\overline{\omega}^4}{240b^5}\lambda_1 \tag{30}$$

$$i = 5, \quad \lambda_7 = \frac{720a^6 - 192a^4b^2\overline{\omega}^2 + 15a^2b^4\overline{\omega}^4 - b^6\overline{\omega}^6}{5040b^6}\lambda_1 \tag{31}$$

The boundary condition at $\xi = 1 - \gamma = 1$ implies

$$\frac{d\phi}{d\xi}(1) = \sum_{i=0}^{\infty} i\lambda_i 1^{i-1} = 0 \tag{32}$$

Eq. (32) constitutes the frequency equation of the clamped-free tapered rod.

As an example, let us consider the following area function:

$$A(\gamma,\xi)=A(0,\xi)=-\xi+2 \tag{33}$$

Substituting the values of λ from Eqs. (25)–(31) into Eq. (32), the following expression is obtained:

$$\left(-\frac{1}{720}\overline{\omega}^6+\frac{19}{320}\overline{\omega}^4-\frac{253}{320}\overline{\omega}^2+\frac{127}{64}\right)\lambda_1=0 \tag{34}$$

For $\lambda_1\neq 0$, the equation in parentheses must vanish

$$-\frac{1}{720}\overline{\omega}^6+\frac{19}{320}\overline{\omega}^4-\frac{253}{320}\overline{\omega}^2+\frac{127}{64}=0 \tag{35}$$

Eq. (35) has the following roots:

$$\begin{gathered}-4.5147\pm 0.7911j\\ 4.5147\pm 0.7911j\\ \pm 1.7993\end{gathered} \tag{36}$$

where $j=\sqrt{-1}$. The positive real root 1.7993 represents an approximation of the first natural frequency of the system. Complex roots have to be discarded. The accuracy of the approximation and number of estimated natural frequencies can be improved using more terms of the series expansion, as shown in Table 1.

Setting $\lambda_1=1$ and substituting $\overline{\omega}=1.7993$ into Eqs. (27)–(31), the corresponding mode shape coefficients are obtained

$$\phi(\xi)=-0.0044\xi^7+0.0085\xi^6+0.0526\xi^5-0.1036\xi^4-0.4562\xi^3+1/4\xi^2+\xi+0 \tag{37}$$

Higher mode shapes can be determined using this iterative procedure. As Table 1 demonstrates, the computation of higher natural frequencies requires increasing orders of the series expansion and the number of estimated frequencies obtained using this method varies with the degree of the approximation n. A larger value of n does not always imply a larger number of estimated frequencies. In all cases, this number is significantly smaller than the degree n. This is a disadvantage of the power series method application to modal analysis that is not frequently mentioned in published research.

2.2. Differential transformation method

The DTM was introduced by Zhou [7] for the solution of linear and non-linear initial value problems in electric circuit analysis. Unfortunately, the authors have not found an available translation of that work (written in Chinese). The following description of the method is based on the work of Chen and Ho [10] who applied the DTM to the solution of eigenvalue problems.

The differential transformation of a function $\phi(\xi)$ is defined as

$$\boldsymbol{\Phi}(k)=\frac{1}{k!}\left[\frac{d^k\phi(\xi)}{d\xi^k}\right]_{\xi=0} \tag{38}$$

where $\Phi(k)$ is the transformed function. The inverse differential transformation of $\Phi(k)$ is as follows:

$$\phi(\xi)=\sum_{k=0}^{\infty}\xi^k\boldsymbol{\Phi}(k) \tag{39}$$

Table 1
Positive real roots computed for the tapered rod (clamped-free model, $\gamma=0$).

Degree n	$\overline{\omega}_1$	$\overline{\omega}_2$	$\overline{\omega}_3$	$\overline{\omega}_4$
7	1.7993	–	–	–
8	1.7949	–	–	–
9	1.7948	4.7707	–	–
10	1.7945	4.4036	–	–
11	1.7942	4.7647	6.3904	–
12	1.7941	–	–	–
13	1.7941	4.8128	–	–
14	1.7940	4.7842	–	–
15	1.7940	4.8005	7.6712	–
16	1.7940	4.8038	6.9830	–
17	1.7940	4.8022	7.8337	8.7961
18	1.7940	4.8019	–	–
19	1.7940	4.8020	7.9573	–
20	1.7940	4.8021	7.7733	–
21	1.7940	4.8021	7.8987	10.3971

Combining Eqs. (38) and (39)

$$\phi(\xi)=\sum_{k=0}^{\infty}\frac{1}{k!}\left[\frac{d^k\phi(\xi)}{d\xi^k}\right]_{\xi=0}\xi^k \tag{40}$$

Eq. (40) shows that the differential transformation is based on the Taylor series expansion of $\phi(\xi)$ at $\xi=0$.

In practical applications, the function $\phi(\xi)$ is expressed by a truncated series, therefore, Eq. (40) becomes

$$\phi(\xi)=\sum_{k=0}^{m}\xi^k\boldsymbol{\Phi}(k) \tag{41}$$

The number of terms in Eq. (41) is determined by convergence requirements. In this method, the following convention is usually adopted: lower-case letters denote original functions, while the corresponding upper-case letters represent their transformed functions.

As indicated in [10], the differential transformation satisfies the properties listed in Table 2.

Zeng and Bert [11] applied the DTM to the free longitudinal vibration analysis of a free-clamped rod with an area function $A(0,\xi)=2\xi$. The case of a clamped-free rod with a general linearly varying area $A(0,\xi)=a\xi+b$ is presented hereafter.

Using the properties in Table 1, the differential transformation of Eq. (7) becomes

$$\begin{aligned}&a\sum_{l=0}^{k}\delta(l-1)(k-l+1)(k-l+2)\boldsymbol{\Phi}(k-l+2)+b(k+1)(k+2)\boldsymbol{\Phi}(k+2)\\&\quad+a(k+1)\boldsymbol{\Phi}(k+1)+a\overline{\omega}^2\sum_{l=0}^{k}\delta(l-1)\boldsymbol{\Phi}(k-l)+b\overline{\omega}^2\boldsymbol{\Phi}(k)=0\end{aligned} \tag{42}$$

Expressing Eq. (42) as a recurrence relation, for $b\neq0$

$$\boldsymbol{\Phi}(k+2)=\frac{-b\overline{\omega}^2\boldsymbol{\Phi}(k)-a\sum_{l=0}^{k}\left[\delta(l-1)(k-l+1)(k-l+2)\boldsymbol{\Phi}(k-l+2)+\overline{\omega}^2\delta(l-1)\boldsymbol{\Phi}(k-l)\right]-a(k+1)\boldsymbol{\Phi}(k+1)}{b(k+1)(k+2)} \tag{43}$$

Evaluating Eq. (43) for $k=0$

$$\boldsymbol{\Phi}(2)=\frac{-a\boldsymbol{\Phi}(1)-b\overline{\omega}^2\boldsymbol{\Phi}(0)}{2b} \tag{44}$$

Then, for $k\geq1$

$$\boldsymbol{\Phi}(k+2)=-\frac{a(k+1)^2\boldsymbol{\Phi}(k+1)+b\overline{\omega}^2\boldsymbol{\Phi}(k)+a\overline{\omega}^2\boldsymbol{\Phi}(k-1)}{b(k+1)(k+2)} \tag{45}$$

Note that Eqs. (44) and (45) are the same recurrence relations given by Eqs. (23) and (24).

For the clamped-free example, the boundary conditions (8) and (9) impose

$$\phi(-\gamma)=\phi(0)=0\rightarrow\boldsymbol{\Phi}(0)=0 \tag{46}$$

$$\frac{d\phi}{d\xi}(1-\gamma)=\frac{d\phi}{d\xi}(1)=0\rightarrow\sum_{k=0}^{\infty}k\boldsymbol{\Phi}(k)1^{k-1}=0 \tag{47}$$

Note that Eqs. (44)–(47) are equivalent to Eqs. (23)–(25) and (32). The natural frequencies and mode shapes can be determined in an iterative way, using the same procedure outlined in Section 2.1.

Table 2
Properties of the differential transformation.

Original function	Transformed function
$w(\xi)=y(\xi)\pm z(\xi)$	$W(k)=Y(k)\pm Z(k)$
$z(\xi)=\beta y(\xi)$	$Z(k)=\beta Y(k)$
$z(\xi)=\frac{d^n y(\xi)}{d\xi^n}$	$Z(k)=(k+1)(k+2)\cdots(k+n)Y(k+n)$
$w(\xi)=y(\xi)z(\xi)$	$W(k)=\sum_{l=0}^{k}Y(l)Z(k-l)$
$w(\xi)=\xi^m$	$W(k)=\delta(k-m)=\begin{cases}1 & \text{if } k=m\\0 & \text{if } k\neq m\end{cases}$

2.3. Matrix implementation of power series

Denote by $\mathcal{P}_n$ the space of polynomials of degree less than or equal to n with ordered basis $\{\xi^n, \xi^{n-1}, \xi^{n-2}, \dots, 1\}$. Given a differential equation, we obtain the matrix representation of its associated differential operator, when the domain and range are restricted to $\mathcal{P}_n$. The following matrix operators are used to write down this differential operator.

Derivative operator

The matrix of the derivative operator is

$$\mathbf{D}^g = \begin{bmatrix} 0 & \cdots & \cdots & \cdots & \cdots & 0 \\ n & \ddots & & & & \vdots \\ \vdots & n-1 & \ddots & & & \vdots \\ \vdots & & \ddots & \ddots & & \vdots \\ \vdots & & & \ddots & \ddots & \vdots \\ 0 & \cdots & \cdots & \cdots & 1 & 0 \end{bmatrix}^g, \quad \text{size} : (n+1)\times(n+1) \tag{48}$$

where g is the order of differentiation. Note that $\mathbf{D}^0$ is the identity matrix $\mathbf{I}$.

Truncated multiplication operator

The multiplication of $\mathbf{D}^g$ by ξ is obtained as $[\mathbf{M_T}]\,[\mathbf{D}]^g$, where $\mathbf{M_T}$ is the "truncated multiplication" operator

$$\mathbf{M_T} = \begin{bmatrix} 0 & 1 & 0 & \cdots & \cdots & 0 \\ \vdots & \ddots & 1 & 0 & & \vdots \\ \vdots & & \ddots & 1 & \ddots & \vdots \\ \vdots & & & \ddots & \ddots & 0 \\ \vdots & & & & \ddots & 1 \\ 0 & \cdots & \cdots & \cdots & \cdots & 0 \end{bmatrix}, \quad \text{size} : (n+1)\times(n+1) \tag{49}$$

Here we see the restriction of the range to $\mathcal{P}_n$, because $\deg(\xi\mathbf{D}^g) = 1+\deg(\mathbf{D}^g) = 1+n$ and only terms of degree less than or equal to n are considered. To multiply by ξ^m, use $\mathbf{M}_\mathbf{T}^m$, and when $m=0$, $\mathbf{M}_\mathbf{T}^0 = \mathbf{I}$.

Using Eqs. (48) and (49), the differential operator associated with the mode shape equation (7) is written as an algebraic system of equations

$$[(a\mathbf{M_T}+b\mathbf{I})\mathbf{D}^2 + a\mathbf{D}^1 + \overline{\omega}^2(a\mathbf{M_T}+b\mathbf{I})] \begin{bmatrix} \lambda_n \\ \lambda_{n-1} \\ \vdots \\ \lambda_0 \end{bmatrix} = \begin{bmatrix} 0 \\ 0 \\ \vdots \\ 0 \end{bmatrix} \tag{50}$$

When the degree is $n=7$, the following equation is obtained:

$$\begin{bmatrix} 2\overline{\omega}^2 & -\overline{\omega}^2 & 0 & 0 & 0 & 0 & 0 & 0 \\ -49 & 2\overline{\omega}^2 & -\overline{\omega}^2 & 0 & 0 & 0 & 0 & 0 \\ 84 & -36 & 2\overline{\omega}^2 & -\overline{\omega}^2 & 0 & 0 & 0 & 0 \\ 0 & 60 & -25 & 2\overline{\omega}^2 & -\overline{\omega}^2 & 0 & 0 & 0 \\ 0 & 0 & 40 & -16 & 2\overline{\omega}^2 & -\overline{\omega}^2 & 0 & 0 \\ 0 & 0 & 0 & 24 & -9 & 2\overline{\omega}^2 & -\overline{\omega}^2 & 0 \\ 0 & 0 & 0 & 0 & 12 & -4 & 2\overline{\omega}^2 & -\overline{\omega}^2 \\ 0 & 0 & 0 & 0 & 0 & 4 & -1 & 2\overline{\omega}^2 \end{bmatrix} \begin{bmatrix} \lambda_7 \\ \lambda_6 \\ \lambda_5 \\ \lambda_4 \\ \lambda_3 \\ \lambda_2 \\ \lambda_1 \\ \lambda_0 \end{bmatrix} = \begin{bmatrix} 0 \\ 0 \\ 0 \\ 0 \\ 0 \\ 0 \\ 0 \\ 0 \end{bmatrix} \tag{51}$$

The boundary conditions provide two additional linearly independent equations to this system

$$\phi(-\gamma) = \phi(0) = 0 \rightarrow \lambda_0 = 0 \tag{52}$$

$$\frac{d\phi}{d\xi}(1-\gamma) = \frac{d\phi}{d\xi}(1) = 0 \rightarrow 7\lambda_7 + 6\lambda_6 + 5\lambda_5 + 4\lambda_4 + 3\lambda_3 + 2\lambda_3 + 1\lambda_1 + 0\lambda_0 = 0 \tag{53}$$

In order to consider $n+1$ equations (to define a square matrix), the first two rows in Eq. (51) – corresponding to higher orders of the approximation – are replaced by the boundary conditions (52) and (53)

$$\begin{bmatrix} 0 & 0 & 0 & 0 & 0 & 0 & 0 & 1 \\ 7 & 6 & 5 & 4 & 3 & 2 & 1 & 0 \\ 84 & -36 & 2\overline{\omega}^2 & -\overline{\omega}^2 & 0 & 0 & 0 & 0 \\ 0 & 60 & -25 & 2\overline{\omega}^2 & -\overline{\omega}^2 & 0 & 0 & 0 \\ 0 & 0 & 40 & -16 & 2\overline{\omega}^2 & -\overline{\omega}^2 & 0 & 0 \\ 0 & 0 & 0 & 24 & -9 & 2\overline{\omega}^2 & -\overline{\omega}^2 & 0 \\ 0 & 0 & 0 & 0 & 12 & -4 & 2\overline{\omega}^2 & -\overline{\omega}^2 \\ 0 & 0 & 0 & 0 & 0 & 4 & -1 & 2\overline{\omega}^2 \end{bmatrix} \begin{bmatrix} \lambda_7 \\ \lambda_6 \\ \lambda_5 \\ \lambda_4 \\ \lambda_3 \\ \lambda_2 \\ \lambda_1 \\ \lambda_0 \end{bmatrix} = \begin{bmatrix} 0 \\ 0 \\ 0 \\ 0 \\ 0 \\ 0 \\ 0 \\ 0 \end{bmatrix} \tag{54}$$

The existence of non-trivial solutions to Eq. (54) implies that the coefficient matrix, which is denoted by $\mathbf{P}_n(\overline{\omega})$, must be singular. Therefore

$$\det[\mathbf{P}_7(\overline{\omega})] = 0 \rightarrow 322{,}560\overline{\omega}^6 - 13{,}789{,}440\overline{\omega}^4 + 183{,}617{,}280\overline{\omega}^2 - 460{,}857{,}600 = 0 \tag{55}$$

Eq. (55) represents the frequency equation of the power series approximation. Note that Eqs. (35) and (55) are equivalent expressions (Eq. (55) can be obtained multiplying Eq. (35) by $-232{,}243{,}200$), therefore, they have the same roots given by Eq. (36).

The corresponding mode shape is obtained finding the non-zero coefficients λ_i of a vector $\boldsymbol{\lambda}$, which satisfies the linear homogenous equation

$$[\mathbf{P}_7(1.7993)]\ \boldsymbol{\lambda} = \mathbf{0} \tag{56}$$

The accuracy of the computation can be improved by increasing the degree of the operator $\mathbf{P}_n(\overline{\omega})$.

2.4. Comparison between the "clamped-free" and "free-clamped" models

The clamped-free rod example defined by Eq. (33) can be solved as the free-clamped model of Fig. 1b, using the following area function:

$$A(\gamma,\xi) = A(0,\xi) = \xi + 1 \tag{57}$$

Since $|b| = |a|$, according to Eq. (14), $R=1$. The element domain equals the convergence interval, so the existence of a series solution centred on the left edge of the element ($\gamma=0$) must be investigated.

The boundary conditions (10) and (11) impose

$$\frac{d\phi}{d\xi}(-\gamma) = \frac{d\phi}{d\xi}(0) = 0 \rightarrow \lambda_1 = 0 \tag{58}$$

$$\phi(1-\gamma) = \phi(1) = 0 \rightarrow \sum_{i=0}^{n} \lambda_i = 0 \tag{59}$$

We construct the system of Eq. (50) for $n=7$ using the area function (57) and substitute the first two rows of the coefficient matrix with the boundary conditions (58) and (59):

$$\begin{bmatrix} 0 & 0 & 0 & 0 & 0 & 0 & 1 & 0 \\ 1 & 1 & 1 & 1 & 1 & 1 & 1 & 1 \\ 42 & 36 & \overline{\omega}^2 & \overline{\omega}^2 & 0 & 0 & 0 & 0 \\ 0 & 30 & 25 & \overline{\omega}^2 & \overline{\omega}^2 & 0 & 0 & 0 \\ 0 & 0 & 20 & 16 & \overline{\omega}^2 & \overline{\omega}^2 & 0 & 0 \\ 0 & 0 & 0 & 12 & 9 & \overline{\omega}^2 & \overline{\omega}^2 & 0 \\ 0 & 0 & 0 & 0 & 6 & 4 & \overline{\omega}^2 & \overline{\omega}^2 \\ 0 & 0 & 0 & 0 & 0 & 2 & 1 & \overline{\omega}^2 \end{bmatrix} \begin{bmatrix} \lambda_7 \\ \lambda_6 \\ \lambda_5 \\ \lambda_4 \\ \lambda_3 \\ \lambda_2 \\ \lambda_1 \\ \lambda_0 \end{bmatrix} = \begin{bmatrix} 0 \\ 0 \\ 0 \\ 0 \\ 0 \\ 0 \\ 0 \\ 0 \end{bmatrix} \tag{60}$$

The frequency equation becomes

$$\det[\mathbf{P}_7(\overline{\omega})] = 0 \rightarrow -2880\overline{\omega}^6 + 99{,}360\overline{\omega}^4 - 1{,}343{,}520\overline{\omega}^2 + 3{,}628{,}800 = 0 \tag{61}$$

Eq. (61) has the following roots:

$$\begin{gathered} 4.1466 \pm 1.3067j \\ -4.1466 \pm 1.3067j \\ \pm 1.8780 \end{gathered} \tag{62}$$

Note that the approximation of the first natural frequency ($\overline{\omega}_1 = 1.8780$) differs significantly from the result obtained for the clamped-free rod ($\overline{\omega}_1 = 1.7992$). The rate of convergence of both models can be analysed using the results listed in Table 3.

As Table 3 illustrates, the clamped-free model stabilises quickly, while the convergence of the free-clamped version is extremely slow even computing the fundamental natural frequency. The computation of higher natural frequencies using the latter model would require extremely large degrees, resulting in a problem that would be too expensive computationally.

This free-clamped example represents a limiting case between the success and failure of the series expansion centred on the left edge of the element (γ=0). As a matter of fact, a steeper slope in the area function (57) would impose

$$a > 1 \rightarrow |a| > |b| \rightarrow R < 1 \tag{63}$$

Then, the interval of convergence would not contain the element boundaries causing the PSM to give meaningless results.

2.5. Selection of the centre of expansion

The speed of convergence of a power series approximation is, in general, very sensitive to the distance from the centre of expansion. If we choose the centre of expansion on one edge of the element, the points closer to the other edge may experience slow convergence. Choosing the centre of expansion to coincide with the centre of the element (γ=1/2) minimises the maximum distance between the points under consideration and the centre of expansion. This means that this choice has a better chance of faster convergence overall.

If the origin of the coordinate system is placed at γ=1/2, the area functions (33) and (57) become

$$A(\gamma,\xi) = A(1/2,\xi) = -\xi + \frac{3}{2}, \quad \text{clamped-free model} \tag{64}$$

$$A(\gamma,\xi) = A(1/2,\xi) = \xi + \frac{3}{2}, \quad \text{free-clamped model} \tag{65}$$

According to Eq. (14), both models have the same radius of convergence: R=3/2. Comparing the results of Tables 3 and 4, we see that the speed of convergence of the solution is greatly improved. Note that when γ=1/2, the results for clamped-free and free-clamped examples are identical.

Table 3
Results for $\overline{\omega}_1$: comparison between "clamped-free" and "free-clamped" models (γ=0).

Degree n	Clamped-free model (γ=0)	Free-clamped model (γ=0)
5	1.787376881424038	1.948343381090857
7	1.799262256950063	1.877980005594379
13	1.794067262363255	1.842212513691217
14	1.794039244169542	1.751667896486866
15	1.794025121850327	1.835965764956050
20	1.794011353980687	1.763650488053592
30	1.794010905201035	1.773410102254346
40	1.794010904759122	1.778428453437813
60	1.794010904759122	1.783536220889923
80	1.794010904758689	1.786122928034675
100	1.794010904758689	1.787685291203742
120	1.794010904758688	1.788731136227012
150	1.794010904758689	1.789780375422146

Table 4
Results for $\overline{\omega}_1$: comparison between "clamped-free" and "free-clamped" models (γ=1/2).

Degree n	Clamped-free model (γ=1/2)	Free-clamped model (γ=1/2)
5	1.796864135421148	1.796864135421148
7	1.794220613434518	1.794220613434518
13	1.794011212724370	1.794011212724370
14	1.794010998518423	1.794010998518423
15	1.794010938952015	1.794010938952015
20	1.794010904890254	1.794010904890254
30	1.794010904758691	1.794010904758691
40	1.794010904758688	1.794010904758688
50	1.794010904758688	1.794010904758688

2.6. Proposed method: domain-partition power series

Fig. 2 shows a free-clamped rod divided into s elements of lengths $L_1, L_2, \ldots, L_s$. The partition of the element domain into regions whose lengths L_i satisfy $L_i/L < R$, guarantees the existence of power series solutions in each region. The mode shape approximation becomes a piecewise function defined on subdomains 1, 2, …, s. The subdomain functions are denoted by $\phi^{(1)}(\xi_1)$, $\phi^{(2)}(\xi_2)$, …, $\phi^{(s)}(\xi_s)$, where

$$-\gamma_i \frac{L_i}{L} \le \xi_i \le (1-\gamma_i)\frac{L_i}{L}, \quad i = 1, 2, \ \ldots\ , \ s \tag{66}$$

The power series approximation of the mode shape is a piecewise polynomial, whose coefficients are denoted by $\lambda_{i,t}$, where $t=1, 2, \ldots, s$ indicates the subdomain, and $i=0, 1, \ldots, n$ represents the coefficient degree. The polynomial degree n and the location of the centre of expansion may vary between subdomains.

For the free-clamped model, the following conditions must be satisfied at $\xi_1 = -\gamma_1 L_1/L$ and at $\xi_s = (1-\gamma_s)L_s/L$

$$\frac{d\phi^{(1)}}{d\xi_1}\left(-\gamma_1 \frac{L_1}{L}\right) = 0 \rightarrow \sum_{i=0}^{n} i\lambda_{i,1}\left(-\gamma_1 \frac{L_1}{L}\right)^{i-1} = 0 \tag{67}$$

$$\phi^{(s)}\left((1-\gamma_s)\frac{L_s}{L}\right) = 0 \rightarrow \sum_{i=0}^{n} \lambda_{i,s}\left((1-\gamma_s)\frac{L_s}{L}\right)^{i} = 0 \tag{68}$$

In addition to these boundary conditions, the following continuity conditions are imposed at partition junctions.

Compatibility of displacements

$$\phi^{(t)}\left((1-\gamma_t)\frac{L_t}{L}\right) - \phi^{(t+1)}\left(-\gamma_{t+1}\frac{L_{t+1}}{L}\right) = 0 \rightarrow \sum_{i=0}^{n} \lambda_{i,t}\left((1-\gamma_t)\frac{L_t}{L}\right)^{i} - \sum_{i=0}^{n} \lambda_{i,t+1}\left(-\gamma_{t+1}\frac{L_{t+1}}{L}\right)^{i} = 0, \ \ t = 1, 2, \ \ldots\ , \ s-1 \tag{69}$$

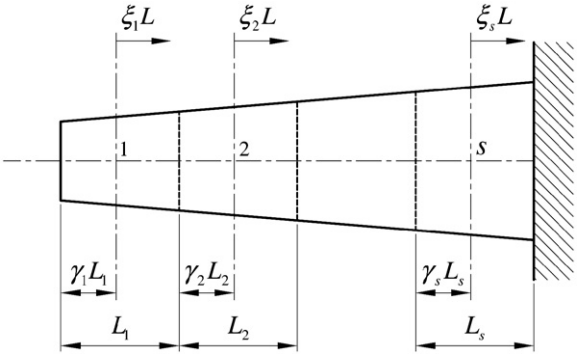

Fig. 2. Free-clamped rod with domain partition.

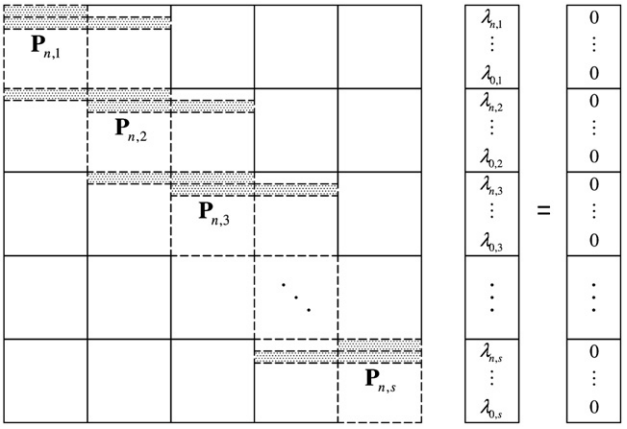

Fig. 3. Form of the differential operator when the element domain is partitioned.

Equilibrium of forces

$$\frac{d\phi^{(t)}}{d\xi_t}\left((1-\gamma_t)\frac{L_t}{L}\right)-\frac{d\phi^{(t+1)}}{d\xi_{t+1}}\left(-\gamma_{t+1}\frac{L_{t+1}}{L}\right)=0\rightarrow\sum_{i=0}^{n}i\lambda_{i,t}\left((1-\gamma_t)\frac{L_t}{L}\right)^{i-1}-\sum_{i=0}^{n}i\lambda_{i,t+1}\left(-\gamma_{t+1}\frac{L_{t+1}}{L}\right)^{i-1}=0,$$

$$t=1,2,\ \ldots\ ,\ s-1 \tag{70}$$

The differential operator associated with the differential Eq. (7) can take the form shown in Fig. 3.

The empty blocks in Fig. 3 represent zero matrices, while the shaded regions indicate assembly of boundary-condition influence coefficients for the elements of vector λ.

Table 5
Power series approximations of the first natural frequency (free-clamped models, $\gamma=0$).

Degree n	Number of domain subdivisions							
	1	2	3	4	5	6	7	8
5	1.9483	1.8072	1.7963	1.7947	1.7943	1.7941	1.7941	1.7940
6	1.7037	1.7884	1.7934	1.7939	1.7940	1.7940	1.7940	1.7940
7	1.8780	1.7967	1.7942	1.7940	1.7940	1.7940	1.7940	
8	1.7248	1.7927	1.7939	1.7940				
9	1.8624	1.7947	1.7940					
10	1.7367	1.7937	1.7940					
11	1.8506	1.7942						
12	1.7453	1.7939						
13	1.8422	1.7941						
14	1.7517	1.7940						
15	1.8360	1.7940						

Table 6
Power series approximations of the first natural frequency (free-clamped models, $\gamma=1/2$).

Degree n	Number of domain subdivisions			
	1	2	3	4
5	1.7969	1.7943	1.7941	1.7940
6	1.7948	1.7940	1.7940	1.7940
7	1.7942	1.7940	1.7940	
8	1.7941			
9	1.7940			
10	1.7940			

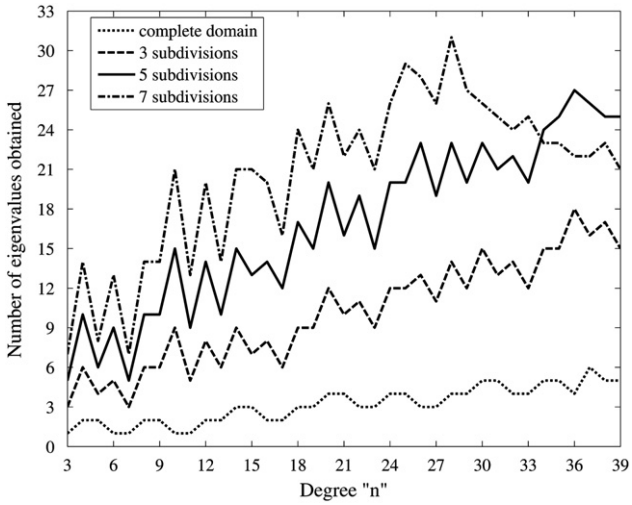

Fig. 4. Number of natural frequencies obtained for several free-clamped models ($\gamma=0$).

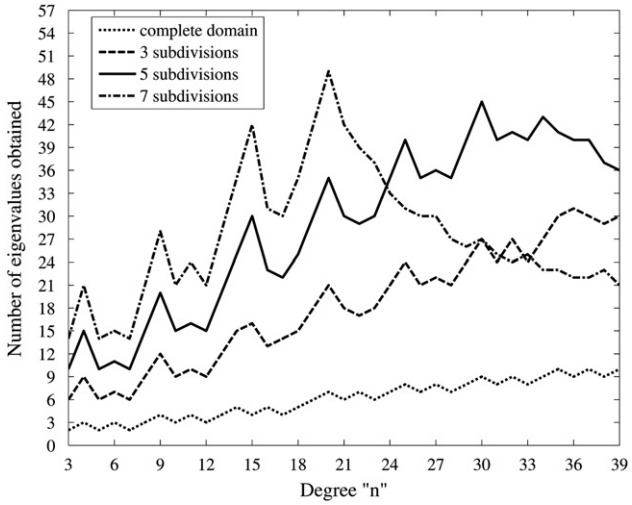

Fig. 5. Number of natural frequencies obtained for several free-clamped models (γ=1/2).

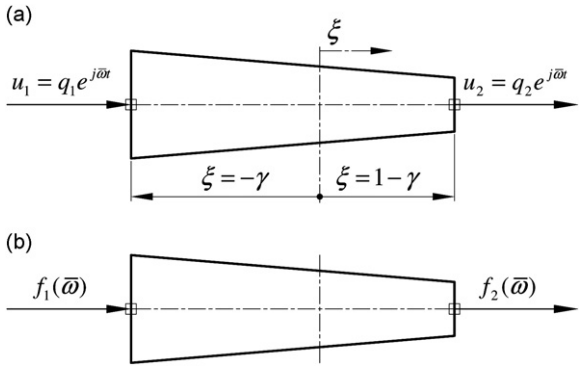

Fig. 6. (a) Non-uniform rod subjected to harmonic end displacements and (b) harmonic forces at the ends of the rod.

The results of Table 5 correspond to free-clamped rods divided into uniform regions and approximated by left-centred polynomials (γ=0) of equal degree in each subdomain. As this table demonstrates, the larger the ratio of R to L_i/L, the faster the series converges. When middle-centred polynomial expansions (γ=1/2) are proposed in each subdomain, the convergence is notably accelerated, as evidenced in Table 6.

The number of eigenvalues obtained varies with the number of subdivisions and the polynomial degree, as Figs. 4 and 5 illustrate. Comparing both figures, we see that when γ=1/2 (Fig. 5), more eigenvalues are captured. In general, the partition of the domain increases the information the model is able to offer.

3. Dynamic stiffness of non-uniform rods

In this section, the computation of dynamic stiffness of a rod subjected to axial vibration is investigated using the classical PSM and the proposed method (Fig. 6).

For the non-uniform rod studied in Section 2, we seek an expression of the form

$$\begin{bmatrix} f_1(\bar{\omega}) \\ f_2(\bar{\omega}) \end{bmatrix} = \begin{bmatrix} S_{11}(\bar{\omega}) & S_{12}(\bar{\omega}) \\ S_{21}(\bar{\omega}) & S_{22}(\bar{\omega}) \end{bmatrix} \begin{bmatrix} u_1(\bar{\omega}) \\ u_2(\bar{\omega}) \end{bmatrix} \tag{71}$$

where the coefficient matrix $S(\bar{\omega})$ is the dynamic stiffness of the rod and relates the Fourier transform of end displacements and the Fourier transform of end forces. For that purpose, consider that the rod is undergoing harmonic forced vibrations produced by the following end displacements (see Fig. 6a)

$$u_1 = u(-\gamma,t) = q_1 e^{j\bar{\omega}t} \tag{72}$$

$$u_2 = u(1-\gamma,t) = q_2 e^{j\bar{\omega}t} \tag{73}$$

q_1 and q_2 are end-displacement amplitudes. The displacements in the rod are governed by the same dimensionless ordinary differential Eq. (4), with displacement boundary conditions $\phi(-\gamma)=u_1$ and $\phi(1-\gamma)=u_2$.

By applying unit displacements at the element ends, and then computing the corresponding axial forces, the coefficients of the dynamic stiffness of the rod are computed. Impose $u_1=0$ and $u_2=1$ and, for a given value of the dimensionless frequency $\overline{\omega}$, solve the boundary value problem to obtain the shape function $\phi(\xi)$. Then, the forces at the ends of the rod are

$$f_1 = -EA(-\gamma)\frac{d\phi}{d\xi}(-\gamma) = S_{12}(\overline{\omega}) \tag{74}$$

$$f_2 = EA(1-\gamma)\frac{d\phi}{d\xi}(1-\gamma) = S_{22}(\overline{\omega}) \tag{75}$$

Similarly, imposing $u_1=1$ and $u_2=0$, $S_{11}(\overline{\omega})$ and $S_{21}(\overline{\omega})$ are obtained.

To illustrate this procedure, we consider the clamped-free rod of Fig. 1a. In this case, the dynamic stiffness $S(\overline{\omega})$ of the rod reduces to $S_{22}(\overline{\omega})$.

3.1. Solution on a single domain

Using the matrix implementation of the PSM presented in Section 2.3, the process of computing dynamic stiffness coefficients is straightforward. Let us calculate an approximation of $S_{22}(\overline{\omega})$ for $\overline{\omega}=2$, considering $\gamma=1/2$, the area function (64), and a degree $n=7$.

The boundary conditions $u_1=0$ and $u_2=1$ imply

$$u_1 = 0 \rightarrow \phi(-1/2) = 0 \rightarrow \sum_{i=0}^{n} \lambda_i (-1/2)^i = 0 \tag{76}$$

$$u_2 = 1 \rightarrow \phi(1/2) = 1 \rightarrow \sum_{i=0}^{n} \lambda_i (1/2)^i = 1 \tag{77}$$

Assembling the system of Eq. (50) for $n=7$, and replacing the first two equations of this system by the boundary conditions (76) and (77), we obtain

$$\begin{bmatrix} -1/128 & 1/64 & -1/32 & 1/16 & -1/8 & 1/4 & -1/2 & 1 \\ 1/128 & 1/64 & 1/32 & 1/16 & 1/8 & 1/4 & 1/2 & 1 \\ 63 & -36 & 3/2\overline{\omega}^2 & -\overline{\omega}^2 & 0 & 0 & 0 & 0 \\ 0 & 45 & -25 & 3/2\overline{\omega}^2 & -\overline{\omega}^2 & 0 & 0 & 0 \\ 0 & 0 & 30 & -16 & 3/2\overline{\omega}^2 & -\overline{\omega}^2 & 0 & 0 \\ 0 & 0 & 0 & 18 & -9 & 3/2\overline{\omega}^2 & -\overline{\omega}^2 & 0 \\ 0 & 0 & 0 & 0 & 9 & -4 & 3/2\overline{\omega}^2 & -\overline{\omega}^2 \\ 0 & 0 & 0 & 0 & 0 & 3 & -1 & 3/2\overline{\omega}^2 \end{bmatrix} \begin{bmatrix} \lambda_7 \\ \lambda_6 \\ \lambda_5 \\ \lambda_4 \\ \lambda_3 \\ \lambda_2 \\ \lambda_1 \\ \lambda_0 \end{bmatrix} = \begin{bmatrix} 0 \\ 1 \\ 0 \\ 0 \\ 0 \\ 0 \\ 0 \\ 0 \end{bmatrix} \tag{78}$$

The solution of Eq. (78) for $\overline{\omega}=2$, leads to

$$\phi(\xi) = -0.0229\xi^7 - 0.0360\xi^6 + 0.1315\xi^5 + 0.1607\xi^4 - 0.9866\xi^3 - 1.1362\xi^2 + 1.2388\xi + 0.7746 \tag{79}$$

Then, according to Eq. (75)

$$S_{22}(2) = EA(1/2)\frac{d\phi}{d\xi}(1/2) = E \times 1 \times (-0.5252) \tag{80}$$

A plot of (S_{22}/EA) as a function of the dimensionless frequency is shown in Fig. 7. Also included in that figure are cross symbols, which indicate the location of the natural frequencies of the system. Searching for the values of $\overline{\omega}$ for which $S_{22}=0$, represents an alternative way for finding natural frequencies. This method was used by Eisenberger in his study of non-uniform rods [5]; results for the first five natural frequencies of this example can be found in his work.

Two intersections are found, one at $\overline{\omega}=1.7942$ and the other at $\overline{\omega}=4.8226$. To obtain an accurate representation of the dynamic stiffness valid in a wider frequency range, more terms of the series expansion must be taken into account. In theory, there is no limit to the number of terms to be considered. However, the matrix of the differential operator $\mathbf{P}_n(\overline{\omega})$ becomes extremely ill conditioned for combinations of high frequency and high degree in the polynomials, preventing further computations. As Fig. 8 indicates, dynamic stiffness estimation is accurate up to $\overline{\omega}\approx 65$. A similar bound is encountered, when computing natural frequencies using the method outlined in Section 2.3. For this

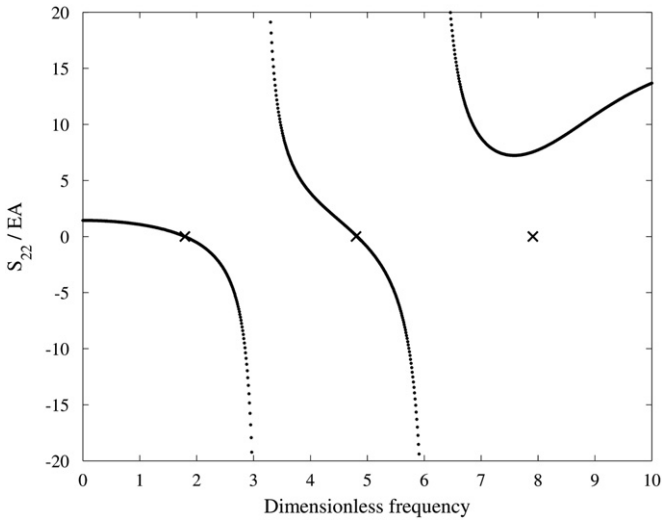

Fig. 7. Dynamic stiffness of a clamped-free rod (single domain, n=7, γ=1/2).

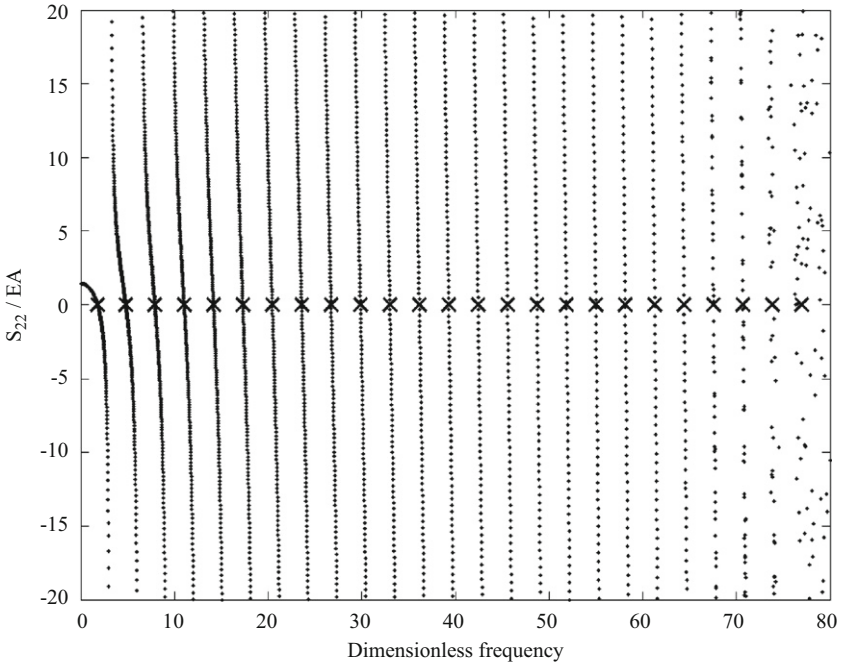

Fig. 8. Dynamic stiffness of a clamped-free rod (single domain, n=130, γ=1/2).

example, numerical difficulties restrict the use of the conventional PSM to calculation of the first twenty-one natural frequencies.

3.2. Solution with domain partition

Apparently, the computational limitation of the standard PSM at high frequency has not been addressed in the literature. Published papers on the application of the PSM to the free vibration analysis of the continuous systems typically show results for the lower five natural frequencies (see for instance Refs. [5,11]).

This computational weakness can be remedied using the PSM with domain partition. This is evidenced in Fig. 9, where the dynamic stiffness of the rod is computed using polynomials of degree n=35 on five uniform subdomains. For this case, thirty-five natural frequencies are captured with excellent precision.

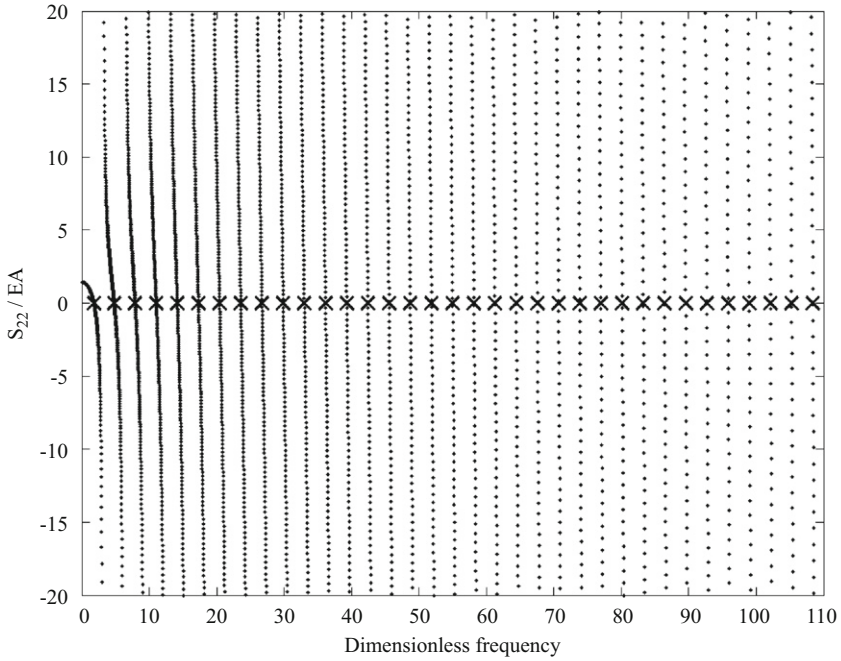

Fig. 9. Dynamic stiffness of a clamped-free rod (five subdomains, $n=35$, $\gamma=1/2$).

4. Concluding remarks and future developments

The classical implementation of power series and the Differential Transformation Method have been compared in this paper. The Differential Transform Method does not differ from the classical power series method and only systematises the computation of recurrence relations for the coefficients of the series expansion, using a different notation. Both versions require extensive symbolic manipulation, while the formulation of power series in terms of matrix operators is easier to systematise and can be implemented in a fully numerical approach, suitable for computer solution.

Two limitations of conventional power series have been addressed: (i) the existence of singularities within the region under analysis may cause the conventional method to fail and (ii) numerical difficulties in the estimation of natural frequencies, mode shapes and dynamic stiffness of continuum models at high frequency. Both limitations are remedied by the proposed domain partition, seeking power series solutions in each interval or subdomain. This simple variation of the power series method augments its range of applicability in the vibration analysis of continuous systems at high frequency. This versatility is gained at an increased computational cost, because the dimension of the matrix operator increases with the number of subdomains required to achieve the desired convergence and accuracy.

The method can be applied in an analogous manner to modal analysis of single displacement field models, such as flexural vibration of beams, torsional vibration of shafts, and lateral vibration of taut strings. The extension of the method to the solution of coupled linear and nonlinear differential equations and the accuracy comparison with traditional finite element methods will be pursued by the authors in future research work.

Acknowledgements

The authors thank Prof. Laura Felicia Matusevich of Texas A&M University; her help and advice during this research are deeply appreciated. Thanks are also due to the reviewers for their valuable comments.

References

[1] G.D. Zill, M.R. Cullen, in: *Differential Equations with Boundary-Value Problems*, Brooks/Cole Publishing Company, California, 2001.
[2] W.E. Boyce, R.C. Diprima, in: *Elementary Differential Equations and Boundary Value Problems*, John Wiley & Sons, New York, 1986.
[3] E. Hairer, S.P. Norsett, G. Wanner, in: *Solving Ordinary Differential Equations I: Nonstiff Problems*, Springer Verlag, Berlin, 2008.
[4] E.L. Ince, in: *Ordinary Differential Equations*, Dover Publications, New York, 1956.
[5] M. Eisenberger, Exact longitudinal vibration frequencies of a variable cross-section rods, *Applied Acoustics* 34 (1991) 123–130.
[6] B. Zhu, A.Y.T. Leung, Dynamic stiffness for thin-walled structures by power series, *Journal of Zhejiang University Science A* 7 (2006) 1351–1357 10.1631/jzus.2006.A1351.

[7] J.K. Zhou, in: *Differential transformation and its application to electrical circuits*, Wuhan Peoples Republic of China: Huazhong University Press, 1986 (in Chinese).
[8] J.P. Boyd, in: *Chebyshev and Fourier Spectral Methods*, Dover Publications, New York, 2001.
[9] R.W. Clough, J. Penzien, in: *Dynamics of Structures*, MacGraw-Hill, New York, 1993.
[10] C.K. Chen, S.H. Ho, Application of differential transformation to eigenvalue problems, *Applied Mathematics and Computation* 79 (1996) 173–188.
[11] H. Zeng, C.W. Bert, Vibration analysis of a tapered bar by differential transformation, *Journal of Sound and Vibration* 242 (2001) 737–739 10.1006/jsvi.2000.3372.